IOP Conf. Series: Materials Science and Engineering **382** (2018) 022062 doi:10.1088/1757-899X/382/2/022062

A Facile Hydrothermal Method to Synthesize Ammonium Tungsten Bronze Nanoplatelets for NIR Absorption

Huiyuan Lu[1], Hua Li*[,1,2], Yujie Chen[1], Hezhou Liu[1,2]

[1]State Key Laboratory of Metal Matrix Composites, School of Materials Science and Engineering, Shanghai Jiao Tong University; [2]Collaborative Innovation Center for Advanced Ship and Deep-Sea Exploration, Shanghai Jiao Tong University. Shanghai 200240, People's Republic of China

Email: lih@sjtu.edu.cn

Abstract. Stable ammonium tungsten bronze (ATB, $(NH_4)_xWO_3$) nanoplatelets with high crystallinity were synthesized via a one-step hydrothermal method without using any organic solvent, in which thiourea was employed as reducing agent and sodium tungstate was used as the starting material. The microstructure, phase and optical properties were controlled by varying hydrothermal conditions. The as-prepared samples exhibit a platelet-like morphology with a width range of 30-150 nm and length of 0.3-3 μm. The patterns of X-ray photoelectron spectroscopy (XPS) confirmed the presence of mixed valence states of tungsten. To check the optical properties, $(NH_4)_xWO_3$-based films were obtained by uniformly casting its dispersion onto fused silica glass substrates. The films exhibited excellent near-infrared light (NIR) absorption abilities by selectively cut-off NIR region by 66.6% (transmittance decreased from 93% of a bare substrate to 26.4% of the films), while maintaining a high visible transmittance of 64.5%, promising its high potential for applications like solar light control filters.

1. Introduction

Near-infrared (NIR, wavelength of 780-2500 nm) light accounts for up to 52% of the photo-energy of sunlight and can be perceived as heat energy by human body [1, 2]. Hence, it is very essential to develop transparent solar heat-shielding filters for windows of buildings and automobiles, which could not only cut off the NIR light but also retain a high visible transparency [3, 4, 19, 21]. Therefore, as the solar filters could help prohibit the temperature rise in summer and achieve a heat insulation in winter, one can reduce the emission of carbon dioxide by saving the energy consumption of air-conditioners.

It has been reported that hexagonal tungsten bronze nanoparticles consisting of mixed chemical valence tungsten ions (W^{5+} and W^{6+}) could exhibit excellent NIR shielding abilities in a wide range of 800-2500 nm [5-7]. Hexagonal tungsten bronze is generally represented by M_xWO_3 (M=Li, K, NH_4^+, etc.), and has an interesting tunnel structure [8,9], in which the guest cations 'M' are embedded in one of corner-linked WO_6 octahedra's two types of channels (Figure 1) [4, 9, 10]. Hydrogen and small alkali metal ions like Li^+ could occupy the narrow trigonal channels, whereas larger cations like NH_4^+ could only take up the hexagonal ones [11].

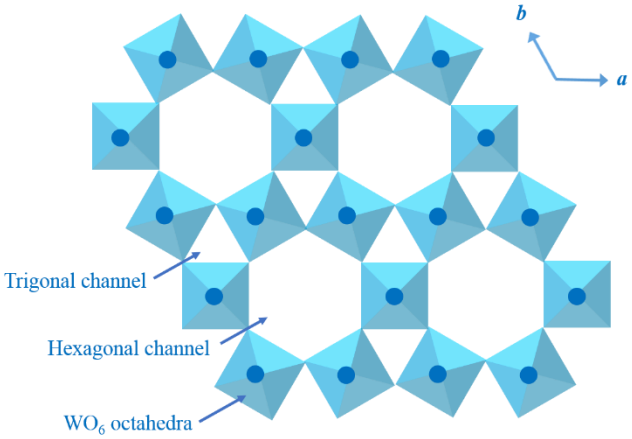

Figure 1 Polyhedral representation of hexagonal M_xWO_3 projected on a-b planes

For the practical applications of hexagonal tungsten bronze, high free electron density is regarded to be vital to exhibit outstanding NIR shielding properties [12, 13, 18]. Further, particle size control is also crucial for visible transparency as the products with featured size well below the wavelength of visible light (380-780 nm) could effectively ensure a clear vision [14, 15]. Different synthesis methods have been applied to obtain hexagonal tungsten bronzes. H. Takeda et al. successfully produced $Na_{0.75}WO_3$ with a size range of 0.1-5 μm by solid state reaction [16]. J. Lee et al. also used a molten-salt route to get three kinds of hexagonal tungsten bronzes crystals [17]. However, the processes of solid state reaction usually involve very high temperature and emission of poisonous gases. Besides, the particles synthesized in this way tend to aggregate, resulting in a larger particle size. Therefore, alternative routes have been employed, i.e. solvothermal and hydrothermal routes. C. Guo et al. fabricated one-dimensional $(NH_4)_xWO_3$ nano-rods with 120 nm in diameter via a solvothermal method [1], but the lengths of the nano-rods were mostly more than 2μm. J. Zhang et al. also obtained nano-sized WO_{3-x} by using oleylamine as reducing agent [17], which is expensive, volatile and inflammable [4, 18].

In this work, a one-step hydrothermal method without using any organic solvent for synthesizing ammonium tungsten bronze (ATB, $(NH_4)_xWO_3$) nanoplatelets was reported. The influences of reaction temperature on the phase, microstructure and optical properties were systematically investigated.

2. Experimental Part

2.1. Synthesis of ATB Nanoplatelets

Sodium tungstate dehydrate ($Na_2WO_4{\cdot}2H_2O$) and thiourea (CH_4N_2S) were purchased from Aladdin Industrial Corporation and were used directly as the starting materials.

In a typical synthesis, 660 mg ($Na_2WO_4{\cdot}2H_2O$ and 609 mg CH_4N_2S were dissolved into 40 mL deionized water. Afterwards, the pH value of the mixture was adjusted to 3-4 by stepwise dropping 1 mol/L hydrochloric acid (HCl). The solution was then transferred to a 100 mL Teflon-lined autoclave, which was sealed and heated at 220 °C, 240 °C and 260 °C for 24 h. Then, the obtained products in dark blue color were washed with deionized water and absolute ethanol for several times by centrifugation. After that, the precipitation was freeze-dried for 24 h. The samples obtained at different hydrothermal temperature were simply represented by sample-220, sample-240 and sample-260.

2.2 Material Characterization

The morphologies of the sample were observed by Field Emission Scanning Electron Microscopy (FESEM) using JSM-6700F at a 10.0 kV acceleration voltage in the Secondary Electron (SE) mode. X-ray Diffraction (XRD) was performed to check the crystallinity with θ/2θ mode using a Goniometer Ultima IV (185 mm) diffractometer with $K\alpha_1$ line of copper (λ= 1.5418 Å). The chemical state of tungsten in the as-prepared nano-powder was checked with the help of X-ray Photoelectron

Spectroscopy (XPS) using a Kratos AXIS Ultra DLD spectrometer with a monochromatic Al Kα X-ray source. Thermal Gravimetric Analysis (TGA) was recorded on Pyris 1 TGA from 50°C to 900°C in air at a heating rate of 10 °C/min.

2.3 Optical Measurement

The dark blue powder was dispersed ultrasonically in deionized water for 3 h to form a mixture with a solid content equals to 150 mg/mL. Afterwards, an ethanol solution with 10 wt% PVP (K30, average molecule weight = 30,000) was added into the dispersion with a volume ratio of 1:1 to promote the formation of film. The mixture dispersion was then uniformly deposited onto a fused silica substrate by spin coating to form a 10 μm ATB-PVP film and was dried at 120 ℃ for 10 min to fabricate the ATB-PVP composite film. The optical properties of the as-prepared films were measured by Lambda 35 UV/VIS Spectrometer in the wavelength range of 300–2500 nm.

3. Results and Discussions

3.1 Phase Identification

XRD analysis was employed to identify the phase and crystallinity of the products synthesized at different temperatures (Figure 2). It is obvious that the reflections of the samples produced at 220 °C , 240 °C and 260 °C could all be well indexed as hexagonal $(NH_4)_xWO_3$ with crystal lattice parameters of a=0.7388 nm and c= 0.7551 nm (JCPDS Card No. 73-1084). However, the intensity of peaks for sample-220 was very weak, while the peaks of sample-240 exhibit the strongest intensity. This indicates that the crystallinity could be improved by controlling the reaction temperature.

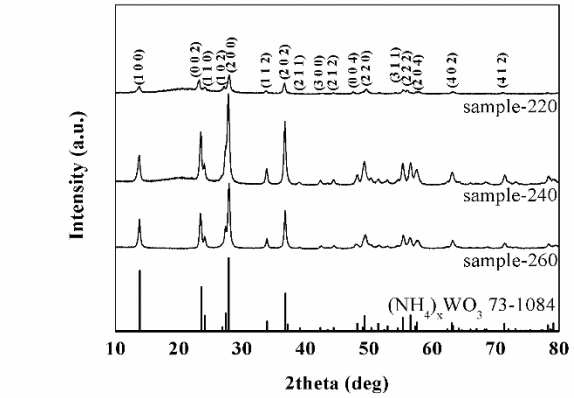

Figure 2 XRD patters of sample-220, sample-240 and sample-260

3.2 Microstructure

Figure 3 shows the SEM images of ATB products synthesized at 220 °C, 240 °C and 260 °C, with various sizes. For the sample obtained at 220 °C (Figure 3-a), the morphology was mostly in the shape of nanoplatelets with an average length around 100 nm and a few up to 400 nm. The widths were around 50nm. As presented in Figure 3-c, the microstructure of sample-240 was plate-like with a length range of 300-600 nm, while the range of width was 30-150 nm. Further, the lengths of these nanoplatelets could reach up to 3 μm if synthesized at 260 °C (Figure 3-f). It should be noted that despite a few nanoplatelets with very large lengths, the rest of sample-260 was still with smaller lengths of 30-100nm (Figure 3-e). Besides, sample-240 possessed the most faceted nanoplatelets, which is in accordance with the highest crystallinity in XRD results.

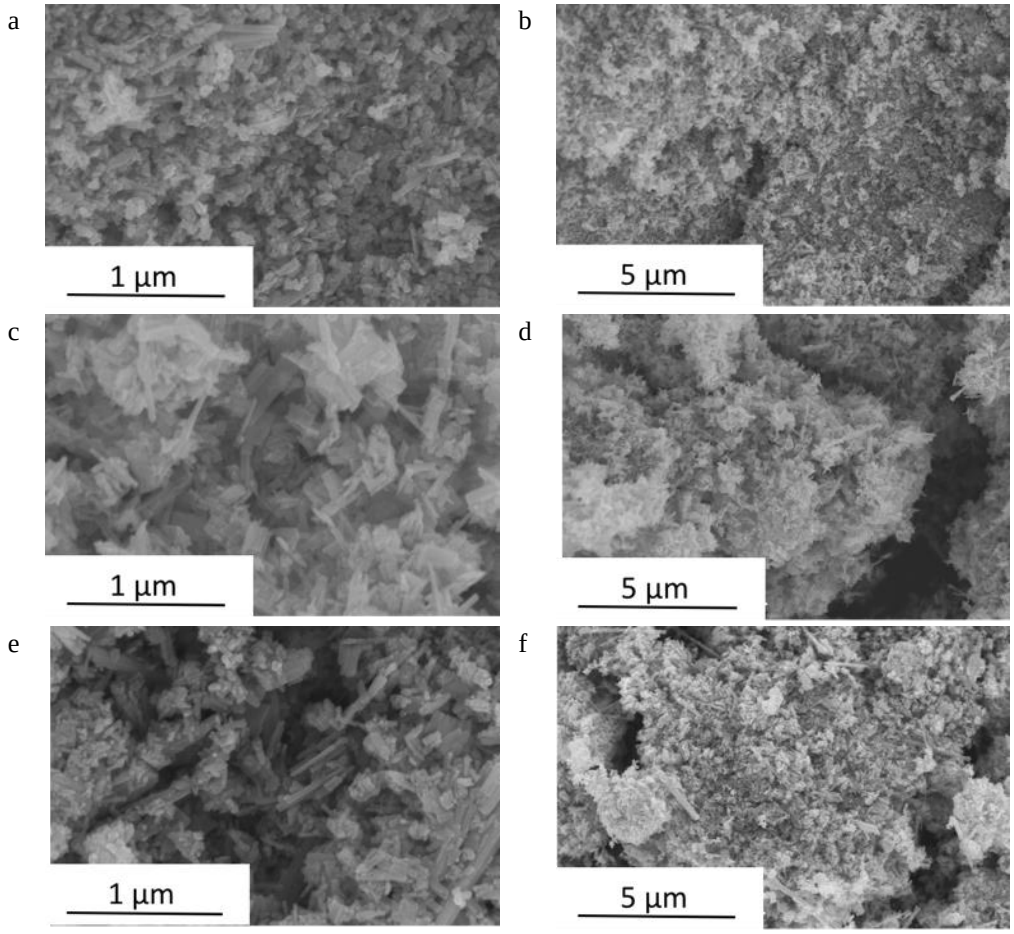

Figure 3 SEM images of sample-220 (a, b), sample-240 (c, d) and sample-260 (e, f)

3.3 XPS Analysis

X-ray photoelectron spectroscopy (XPS) was executed to confirm the chemical composition and valence state of $(NH_4)_xWO_3$ nanocrystals. The high-resolution scan spectrum revealed the existence of elements of N, O, W and C in the sample (Figure 4-a). The presence of C could be attributed to some organic residuals chemically or physically adsorbed during the synthesize process (Figure 4-b). The energy distribution of tungsten core level (W4f) photoelectrons was obtained as shown in Figure 4-c. The spectrum could be well fitted into two spin-orbit doublets, corresponding to two different valence states of tungsten. Two main peaks at 37.6eV and 35.5eV, could be the results from the emission of $W4f_{5/2}$ and $W4f_{7/2}$ core levels from W atoms in an oxidation rate of 6+. As for the second doublets, with lower peaks at 34.2eV for $W4f_{5/2}$ and 36.3eV for $W4f_{7/2}$, might be represented for the W atoms in an oxidation rate of 5+. These analyses for W core level in tungsten bronze are in good agreement with values reported in previous literature [2]. Further, the ratio of NH_4^+/WO_3 was determined to be 0.16 by comparing the integrated areas of nitrogen (N1s) at 401.1eV and tungsten core level (W4f). Therefore, the possible chemical formula of the product could be written as $(NH_4)_{0.16}WO_3$.

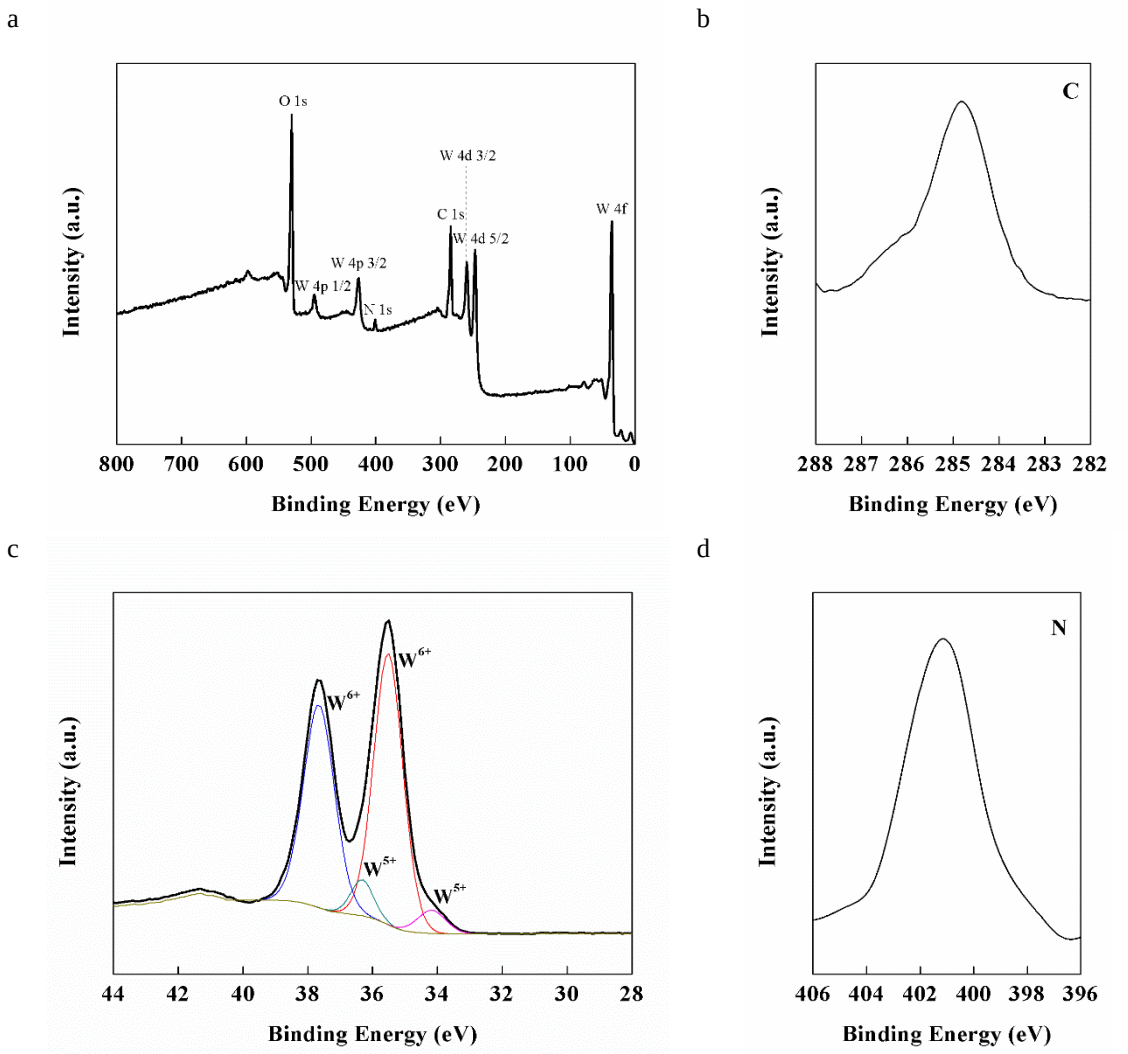

Figure 4 XPS spectra of $(NH_4)_xWO_3$ nanoplatelets: a, full range XPS spectrum; b, XPS spectrum of C1s, XPS spectrum of W4f core level with peaks corresponding W^{6+} and W^{5+} valence states; d, XPS spectrum of N1s

3.4 Thermal Behavior

The thermal behavior of sample-240 was studied by thermogravimetric analysis (TGA) in the air atmosphere from 50 °C to 800 °C with a heating rate of 10 °C/min. From Figure 5, three stages of weight loss could be observed. First of all, the weight loss up to 190 °C could be assigned to the desorption of water, including the elimination of absorbed water (~90 °C) and further loss of structural water (~190 °C). The second stage was from 190 to 380 °C due to the departure of NH_3 as a result of $(NH_4)_xWO_3$'s decomposition. Finally, the subsequent weight loss from 380 to 520 °C might be attributed to the combustion of organics shown in XPS analysis [1]. The weight loss during this stage might also be ascribed to the oxygen deficiency introduced by reducing agent during synthesizing process [20]. No weight loss was observed afterwards and the remaining powder after TGA was confirmed to be monoclinic WO_3 phase by XRD.

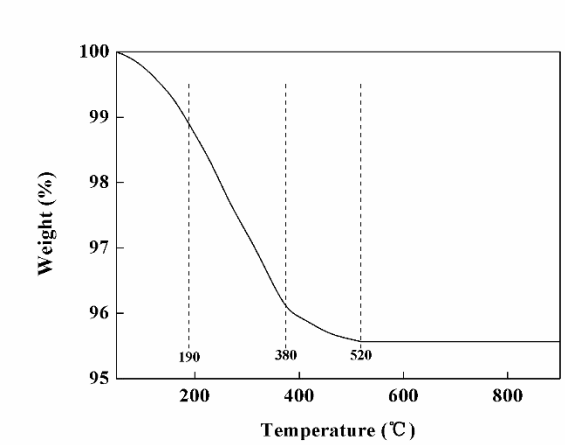

Figure 5 TG plot of $(NH_4)_xWO_3$ nanoplatelets recorded in air at a heating rate of 10°C /min

3.5 Optical Measurement

Figure 6 exhibits the images and transmittance spectra of films composed of the as-prepared $(NH_4)_xWO_3$ nanoplatelets. The coated films were tinted blue but still transparent (Figure 6-a). As shown in Figure 6-b, the films coated by $(NH_4)_xWO_3$ nanoplatelets selectively transmitted the majority of visible light in the range of 380-780 nm, while cutting off near-infrared light (i. e. 780-2500 nm) effectively. As expected, the fused silica substrate without any deposition was highly transparent for both visible and NIR light (transmittance~93%). For the as-prepared samples, the luminous transmittance were still in a good state (43.8％ - 85.2%) and the near-infrared transmittance were decreased with a range of 18.8% - 59.4%.

The NIR shielding properties varied for products synthesized at different temperatures. Sample-240 possessed better NIR shielding effect, but with less visible light transparency, which might be due to the overall larger grain size of its faceted nanoplatelets [4]. Sample-220 and sample-260 did much better in visible transparence because of their relatively smaller particle size. The NIR absorption properties are closely related to the free electrons originating from W^{5+} and W^{6+} [4]. This helps explain why sample synthesized at 240°C and 260°C presented better NIR shielding abilities. Sample-220's poor performance in NIR absorption might be attributed to its low crystallinity.

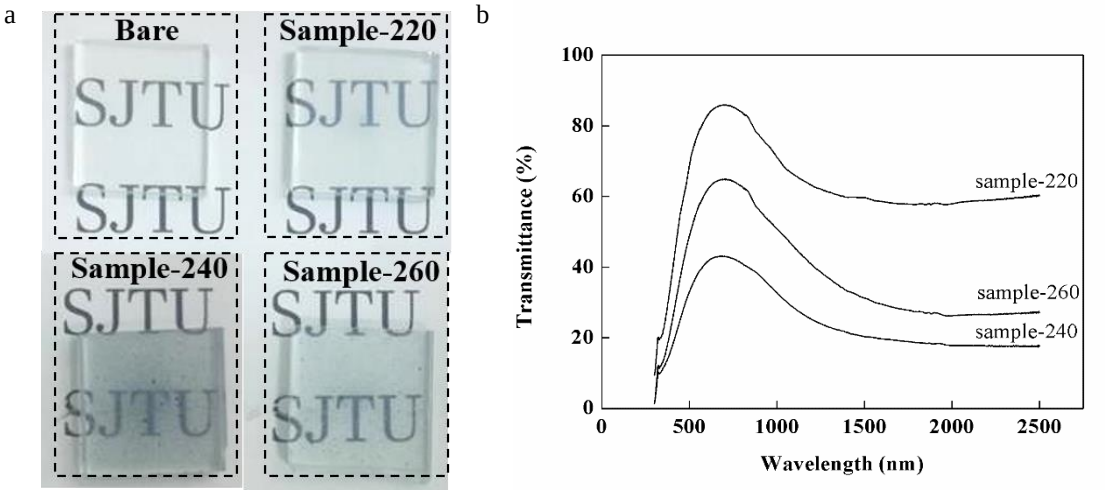

Figure 6 Images and transmittance profiles of films containing sample-220, sample-240 and sample-260

4. Conclusion

In summary, $(NH_4)_xWO_3$ nanoplatelets with width of 30-150 nm and length of 0.3-3 μm were synthesized *via* a facile hydrothermal method without using any organic solvent. It is confirmed that the reaction temperature played an important role in the phase and morphologies of the products. Characterization results proved that the hexagonal tungsten bronze phase with a mixed valence states of W^{5+} and W^{6+}were obtained. Optical measurements presented that the as-prepared $(NH_4)_xWO_3$ nanoparticles synthesized at 260 °C could exhibit high transmittance of visible light (up to 64.5%) as well as strong shielding of NIR light (decreased ~66.6% comparing with bare silica substrates). Thus, the $(NH_4)_xWO_3$ nanoplatelets are promising for applications like solar light control filters, and is also expected to be a candidate for a wide range of applications including photothermal and electrochromic devices.

Acknowledgements

This work is supported by the Natural Science Foundation of China (No. 51373096), Basic Research Field of Shanghai Science and Technology Innovation Program (No. 16JC1401500), Special Zone of Science and Technology Innovation Program Funding (No. 17-163-130-ZT-008-026-01) and Morning Star Young Scholar Award of Shanghai Jiao Tong University (U1733130). Instrumental Analysis Center of Shanghai Jiao Tong University and National Engineering Research Center for Nanotechnology are gratefully acknowledged for assisting with relevant analyses.

References

[1] Guo C, Yin S, Dong Q, Sato T. Simple route to $(NH_4)_xWO_3$ nanorods for near infrared absorption[J]. Nanoscale, 2012, 4: 3394-3398.
[2] Yan M, Gu H, Liu Z, Guo C, Liu S. Effective near-infrared absorbent: ammonium tungsten bronze nanotubes[J]. RSC Advances. 2015, 5: 967-973.
[3] Niklasson GA, Granqvist CG. Electrochromics for smart windows: thin films of tungsten oxide and nickel oxide and devices based on these[J]. Journal of Materials Chemistry. 2007, 17: 127-56.
[4] Kang L, Xu W, Wang K, Liang W, Liu X, Gao F, Lan A, Yang Y, Gao Y. Transparent $(NH_4)_xWO_3$ colloidal dispersion and solar control foils: Low temperature synthesis, oxygen deficiency regulation and NIR shielding ability[J]. Solar Energy Materials and Solar Cells. 2014, 128: 184-189.
[5] Guo C, Yin S, Yan M, Sato T. Facile synthesis of homogeneous Cs_xWO_3 nanorods with excellent low-emissivity and NIR shielding property by a water controlled-release process[J]. Journal of Materials Chemistry. 2011, 21: 5099-5105.
[6] Guo C, Yin S, Yu H, Liu S, Dong Q, Goto T, Zhang Z, Li Y, Sato T. Photothermal ablation cancer therapy using homogeneous Cs_xWO_3 nanorods with broad near-infra-red absorption[J]. Nanoscale. 2013, 5: 6469-6478.
[7] Liu Y, Zhao L, Su J, Li M, Guo L. Fabrication and properties of a branched $(NH_4)_xWO_3$ nanowire array film and a porous WO_3 nanorod array film[J] ACS Applied Materials & Interfaces. 2015, 7: 3532-3538.
[8] Michailovski A, Ragnar Kiebach, Bensch W, Grunwald J-D, Baiker A, Komarneni S. Morphological and Kinetic Studies on Hexagonal Tungstates[J]. Chemistry of Materials.2007, 19: 185-197.
[9] Gao T, Jelle BP. Visible-Light-Driven Photochromism of Hexagonal Sodium Tungsten Bronze Nanorods[J]. The Journal of Physical Chemistry C. 2013, 117: 13753-13761.
[10] [Fouad NE, Nohman AKH, Mohamed MA, Zaki MI, Characterization of ammonium tungsten bronze $[(NH_4)_{0.33}WO_3]$ in the thermal decomposition course of ammonium paratungstate[J], Journal of Analytical and Applied Pyrolysis. 2000, 56: 23-31.
[11] J. Bludska´, I. Jakubec. Insertion of Hydrogen into Hexagonal Tungsten Bronzes $A_{0.3}WO_3$ (A = K, NH_4 and Cs)[J]. Z. Phys. Chem.1996, 194: 69-75.
[12] Xie YP, Liu G, Yin L, Cheng H-M. Crystal facet-dependent photocatalytic oxidation and reduction

reactivity of monoclinic WO_3 for solar energy conversion[J]. Journal of Materials Chemistry.2012, 22: 6746-6751.

[13] Gu Z, Ma Y, Zhai T, Gao B, Yang W, Yao J. A simple hydrothermal method for the large-scale synthesis of single-crystal potassium tungsten bronze nanowires[J] Chemistry. 2006, 12: 7717-7723.

[14] Guo C, Yin S, Zhang P, Yan M, Adachi K, Chonan T. Novel synthesis of homogenous Cs_xWO_3 nanorods with excellent NIR shielding properties by a water controlled-release solvothermal process[J]. Journal of Materials Chemistry. 2010, 20: 8227-8229.

[15] Guo C, Yin S, Huang Y, Dong Q, Sato T. Synthesis of $W_{18}O_{49}$ nanorod via ammonium tungsten oxide and its interesting optical properties[J]. Langmuir. 2011, 27: 12172-12178.

[16] Takeda H, Adachik K. Near infrared absorption of tungsten oxide nanoparticle dispersions[J]. Journal of the American Ceramic Society. 2007, 90: 4059-4061.

[17] Lee J-S, Liu H-C, Peng G-D, Tseng Y. Facile synthesis and structure characterization of hexagonal tungsten bronzes crystals[J]. Journal of Crystal Growth. 2017, 465: 27-33.

[18] Liu B, Yin S, Wu X-Y, Wang Y, Huang Y, Wu J, Sekino T, Matsushita J, Lee S-W, Kobayashi M, Kakihana M, Sato T. Graphene/M_xWO_3 (M = Na, K) nanohybrids with excellent electrical properties[J]. Carbon.2015, 94: 309-316.

[19] Xu X, Zhang W, Hu Y, Wang Y, Lu L, Wang S. Preparation and overall energy performance assessment of wide waveband two-component transparent NIR shielding coatings[J]. Solar Energy Materials and Solar Cells. 2017, 168: 119–129

[20] Wang K, Kang L-T, Chen S, Dong L, Liang `w, Gao F. Effects of reaction temperature on structure and optical properties of hydrothermally prepared $(NH_4)_xWO_{3-y}$ and WO_3•$1/3H_2O$[J]. Journal of Inorganic Materials. 2014, 29: 550-556.

[21] Lee W-H, Hwang H, Moon K, Shin K, Han J-H, Um S-H, Park J, Cho J-H. Increased Environmental Stability of a Tungsten Bronze NIR-absorbing Window[J]. Fibers and Polymers. 2013, 14: 2077-2082.